Int. J. Electrochem. Sci., 15 **(2020)** 8229 – 8240, doi: 10.20964/2020.08.19

International Journal of
ELECTROCHEMICAL
SCIENCE
www.electrochemsci.org

Effect of Sodium Tungstate on the Corrosion Behavior of Fe-Base Alloy in H_2SO_4 Solution

Ghalia A. Gaber[1], *Hayam. A. Aly*[2, 3], *Lamiaa Z. Mohamed*[4,*]

[1] Department of Chemistry, Faculty of Science (Girls), Al-Azhar University, P.O. Box: 11754, Yousef Abbas Str., Nasr City, Cairo, Egypt
[2] Department of Metallurgical and Materials Engineering, Faculty of Petroleum and Mining Engineering, Suez University, P.O. Box 43721, Suez, Egypt
[3] Central Metallurgical Research and Development Institute (CMRDI), P.O. Box 11421, Helwan, Egypt
[4] Mining, Petroleum and Metallurgical Engineering Department, Faculty of Engineering, Cairo University, Egypt
[*]E-mail: lamiaa.zaky@cu.edu.eg

Received: 5 March 2020 / *Accepted:* 30 April 2020 / *Published:* 10 July 2020

The corrosion behavior of Fe-base alloy in H_2SO_4 acid at different concentrations was evaluated. The effect of sodium tungstate inhibitor on Fe-base alloy in 10 % H_2SO_4 solutions was evaluated by using weight loss and potentiodynamic polarization methods along with scanning electron microscope and energy dispersive x-ray analysis. The corrosion rate and surface morphology of Fe-base alloy in the presence of various concentrations of sodium tungstate inhibitor compared to control in 10 % H_2SO_4 solutions were measured. The sodium tungstate inhibitor was found to improve the protection against corrosion in comparison to the uninhibited 10 % H_2SO_4 solution.

Keywords: Corrosion; Protection; Inorganic inhibitor; Electrochemical technique; Microstructure

1. INTRODUCTION

Pickling is commonly used in various manufacturing processes [1-3]. Significant problems rising from corrosion in tubing and oil production machinery often resulted in cracks and breakdown in construction, which have led to accidents. The metal corrosion rate in mineral acids is more expeditious than in other environments, which are mainly used in pickling and removing the FeO layer [4]. The metal protection might be achieved chemically or electrochemically through surface modification by using classical inhibitors [5-10]. The protection is applicable, cost-effective, and commonly used in industrial production. During the protection of metals or alloys from corrosion; a suitable corrosion

inhibitor should be used to decrease the amount of corrosive effect, enhance the pickling effect, and increase the service time. The active agent of these inhibitors is an inorganic anion that protects metal surfaces, including their penetration into the oxide layer, by various mechanisms. Accordingly, decreasing and controlling all causes that lead to an increase in the demand to protect the environment. In turn, this harms and pollutes the surrounding environment and affect drastically the economy [8]. Several countries and regions are issuing several regulatory controls to guide the use and discharge of toxic substances, especially inorganic and heavy metals. Sodium tungstate inhibitor is an eco-friendly inhibitor that decreases the corrosion rate and protects metals [11, 12]. Previous studies have examined the corrosion behavior of mild steel in the presence of sodium tungstate inhibitors but have not studied their effect on the microstructure and the corroded surface [13]. This work aims to explore the effect of sodium tungstate inhibitor with different concentrations in the H_2SO_4 solution on the corrosion characteristics of Fe-base alloy. Additionally, SEM and EDAX were used to explore the effect on the surface morphology of the Fe-base alloy.

2. EXPERIMENTAL WORK

Table 1 gives the chemical composition of the investigated Fe-base alloy. The working electrode was polished before each experiment, washed with deionized H_2O and dried by $(CH_3)_2CO$.

Table 1. Fe-base alloy chemical composition in wt. %

Fe	C	Si	Mn	Cr	Mo	Ni	Cu	Ti	V	W
65.80	0.08	0.74	1.02	16.20	0.34	12.60	0.43	0.09	0.13	2.37

The counter electrode was a platinum sheet while the saturated calomel electrode (SCE), (Hg/Hg_2Cl_2-Sat. KCl), was used as a reference electrode connected to a conventional electrolytic cell of capacity 25 ml of solutions. Measurements of weight loss and potentiodynamic polarization tests were used to evaluate the corrosion protection for the examined Fe-base alloy (as working electrodes) in H_2SO_4 in the presence of the inorganic inhibitor. Weight loss measurements were performed in a glass vessel with 25 ml of H_2SO_4 solution (grade 98% H_2SO_4 acid) with and without the existence of different concentrations of $Na_2WO_4 \cdot 2H_2O$ inhibitor (0.01, 0.03, 0.05, and 0.1 M). The immersion time for the weight loss experiment was 120 hr at 20 ± 1ºC. The average corrosion rate obtained using Eqs. 1 and 2 as follows [14]:

$$\Delta W = W_1 - W_2 \quad (1)$$

$$\text{C.R. (mm/y)} = \frac{\Delta W \times K}{A \times T \times D} \quad (2)$$

where K = a constant (8.76×10^4), T = time of exposure in hours, A = area in cm^2, ΔW = mass loss in grams, and D = density of Fe-base alloy (7.87 g/cm^3). The degree of surface coverage (θ) was provided by Eq. 3:

$$\theta = \frac{W_0 - W_i}{W_0} \quad (3)$$

Where W_i and $W_\circ$ are the values of weight loss of Fe-base alloy in inhibited and uninhibited solutions, respectively. The inhibition efficiency $IE(\%)$ was measured by Eq. 4:

$$IE(\%) = \theta \times 100 \quad (4)$$

Potentiodynamic Fe-base alloy polarization was performed at a scan rate of 0.5 mV/s from –0.8 and +0.8 V. Before starting the test, the working electrode was first submerged in the test solution for 30 min to achieve a steady-state value of the open circuit potential. The corrosion rate (C.R.) was measured in μm consumption of Fe per year according to Faraday's Law as follows Eq. 5:

$$CR\ (\mu m/year) = 3.3 I_{corr} M/zd \quad (5)$$

Where; z = ionic charge (3 for Fe), M = atomic weight of metal (55.85 for Fe), d = density of Fe, 7.87 g/cm^3, and I_{corr} = corrosion current density, μA/cm^2.

Values of I_{corr} and corrosion potential (E_{corr}) were provided from the intersection of the linear anodic and cathodic branches of Tafel curves and were calculated in uninhibited and inhibited solutions with different concentrations of sodium tungstate. Each experiment was repeated at least three times. Degrees of surface coverage (θ) in potentiodynamic measurements were determined using Eq. 6.

$$\theta = 1 - I_{corr}/ I_{corr}^\circ \quad (6)$$

where I_{corr}° and I_{corr} are the corrosion current densities in the uninhibited and inhibited with sodium tungstate solutions, respectively. The inhibitive efficiency (IE %) was measured employing Eq.7

$$IE\ \% = \theta \times 100 \quad (7)$$

Scanning electron microscopy (SEM) and energy dispersive x-ray analysis (EDAX) were used to examine the surface morphology of the corrosion products on the Fe-base alloy after 120 hr immersion in 10% H_2SO_4 solution in the uninhibited and inhibited at various Na_2WO_4 concentrations.

3. RESULTS AND DISCUSSION

3.1 Weight loss measurements

Table 2. Corrosion rate (CR), by weight loss method for corrosion behavior of Fe-base alloy in various concentrations of H_2SO_4 solution

Conc. of H_2SO_4	48 hr		120 hr	
	Wt. loss, (g)	CR, (mm/y)	Wt. loss, (g)	CR, (mm/y)
1%	0.0050	0.5797	0.0080	0.3710
5%	0.0280	3.2465	0.0940	4.3595
10%	0.0425	4.9277	0.1535	7.1191

Fig. 1. demonstrates the weight loss in (g) for corrosion behavior of Fe-base alloy in different concentrations of H_2SO_4 solution at various time intervals at 20 ºC. The corrosion rate (CR) and weight loss for corrosion behavior of Fe-base alloy in various concentration of H_2SO_4 solution are tabulated in Table 2.

The results showed that Fe-base alloy weight loss increased and varied linearly with increasing time and concentrations. During corrosion, the linearity given suggested the absence of insoluble surface film. The reaction rate decreased slightly in low concentrated H_2SO_4 acid, before entering a steady state.

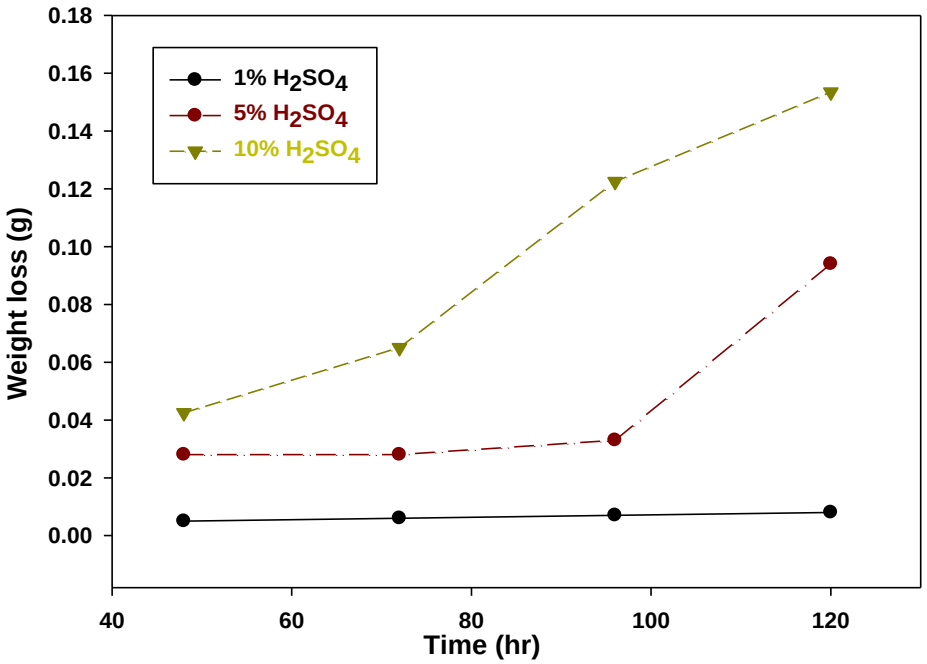

Figure 1. Variation in weight loss with exposure time for corrosion behavior of Fe-base alloy in various concentration of H_2SO_4 solution.

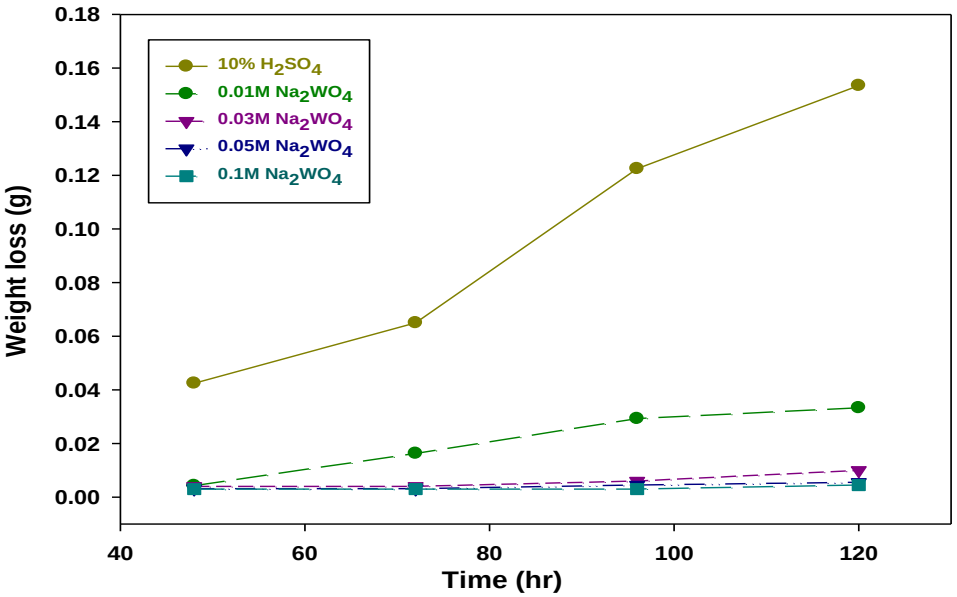

Figure 2. Variation in weight loss with exposure time for Fe-base alloy in 10 % H_2SO_4 solutions in the presence and absence of various concentrations of $Na_2WO_4 \cdot 2H_2O$

Fig. 2. illustrates the variation in weight loss with exposure time for Fe-base alloy in 10 % H_2SO_4 solutions for both uninhibited and inhibited solutions with various concentrations of $Na_2WO_4 \cdot 2H_2O$.

Different parameters such as corrosion rate (CR), Surface coverage (θ), and the inhibition efficiency (IE %) are given in Table 3.

Table 3. Corrosion rate (CR), Surface coverage (θ) and the Inhibition efficiency (IE %) for Fe-base alloy in 10 % H_2SO_4 solutions in the presence and absence of various concentrations of $Na_2WO_4{\cdot}2H_2O$ given by weight loss method at 20ºC

Inhibitor Conc. (M)	Wt. loss, (g)	CR, (mm/y)	θ	*IE*, %
10% H_2SO_4 Blank	0.1535	7.1191	--	--
0.01M Na_2WO_4	0.0333	1.5444	0.783	78
0.03M Na_2WO_4	0.0100	0.4637	0.934	93
0.05M Na_2WO_4	0.0055	0.2551	0.964	96
0. 1M Na_2WO_4	0.0045	0.2087	0.971	97

The results indicated that the weight losses of Fe-base alloy in the presence of Na_2WO_4 were lower than that of inhibitor-free (10 % H_2SO_4 solutions). The inhibitor was reported to be first adsorbed onto the Fe surface and thus impeding the corrosion process [15] because the sodium tungstate is fairly efficient as an inhibitor for Fe-base alloy in 10 % H_2SO_4 solutions. The corrosion rates in the presence of sodium tungstate became low and decreased with time at low inhibitor concentrations (0.01 M). At higher concentrations (0.05 and 0.1 M), the corrosion rates showed little observable change in its values after prolonged immersion time, suggesting a relation to some extent with the duration of immersion. It was noted that a strong reaction (characterized by (H_2) gas bubbles formation) occurred immediately after sample immersion in the acid solutions. The gas evolution rate increased by increasing the concentration of H_2SO_4 acid. The addition of $Na_2WO_4{\cdot}2H_2O$ not only improved the Fe-base alloy's corrosion resistance but also increased the growth rate and surface roughness. Hence, the relation between the corrosion resistance of the Fe-base alloy and the concentration of $Na_2WO_4{\cdot}2H_2O$ was studied. The concentration of 0.1M $Na_2WO_4{\cdot}2H_2O$ showed the best corrosion resistance with a corrosion rate of 0.2087 mm/y and the highest IE 97 %. The anodic polarization plot was correlated with the electrochemical dissolution of a metal substrate, and the cathodic polarization plot was shown to be due to the evolution of cathodic hydrogen during water reduction [16].

3.2 Potentiodynamic polarization measurements

The electrochemical data, namely anodic and cathodic Tafel slopes (β_a and β_c), E_{corr} and I_{corr} derived from the polarization curves, the polarization resistance (R_p) values were determined using Stern–Geary Eq. 8 [17]:

$$R_p = \frac{\beta a \,.\, \beta c}{2.303\ I_{corr}\,(\beta a + \beta c)} \qquad (8)$$

Fig. 3 displays the polarization curves for Fe-base alloy in different concentrations of H_2SO_4 acid solutions. Table 4 provides all the above corrosion parameters obtained for the Fe-base alloy from the Tafel extrapolation method.

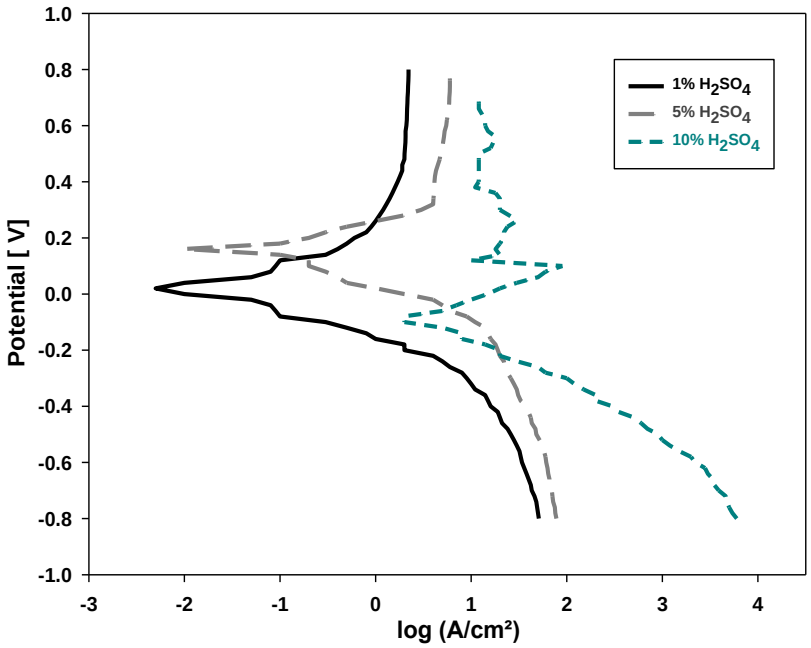

Figure 3. Potentiodynamic polarization curves for Fe-base alloy in different concentration of H_2SO_4 solutions.

Table 4. Corrosion parameters for Fe-base alloy in various concentration of H_2SO_4 acid solutions.

Conc. of H_2SO_4	E_{corr} V	I_{corr} µA/cm^2	β_a V/dec	β_c V/dec	R_p Ωcm^{-2}	*CR*,µm/y
1%	0.020	3.162	0.666	0.440	363.80	24.680
5%	0.160	3.981	0.120	0.480	104.70	31.077
10%	-0.087	11.220	0.150	0.160	2.99	87.580

The results showed that the corrosion currents density, I_{corr}, and the corrosion rate increased with the increase of the concentration of H_2SO_4 acid solutions. The current density of corrosion is one of the important parameters used to measure the materials' resistance to corrosion. The higher the current density of the corrosion, the more severe the material corrosion [18]. From the polarization curves, it can be seen that, after the inhibitors were applied, the current density decreased. The effect of concentrations of Na_2WO_4 (0.01 - 0.1 M) for the Fe-base alloy was studied in 10 % H_2SO_4 solutions. The addition of Na_2WO_4 to the Fe-base alloy in 10 % H_2SO_4 acid solutions (Fig. 4 and Table 5) resulted in a decrease of the free-corrosion current densities (I_{corr}). When the concentration of $Na_2WO_4{\cdot}2H_2O$ was further increased to 0.1 M, the current density was reduced consequently. The lowest corrosion density was found for the concentration of 0.1 M $Na_2WO_4{\cdot}2H_2O$, being 0.039 µA/cm^2, which is significantly lower than that of the blank (10 % H_2SO_4) being (11.220 µA/cm^2). As for the polarization resistance after the addition of 0.1 M sodium tungstate to the Fe-base alloy in 10 %, H_2SO_4 acid solutions, it showed the highest value of corrosion density being 10862.2 Ω.cm^{-2}. The decrease in the current density and accordingly increase in resistance to polarization in the presence of the inhibitor is largely due to the effect of the formed protective layer in combating the detrimental effect of pores and cracks

within the inhibitor, making it more difficult for the corrosive media to transport. The corrosion rate of the Fe-base alloy is diminished by increasing Na_2WO_4 concentrations as seen in Fig. 4 and viewed in Table 5.

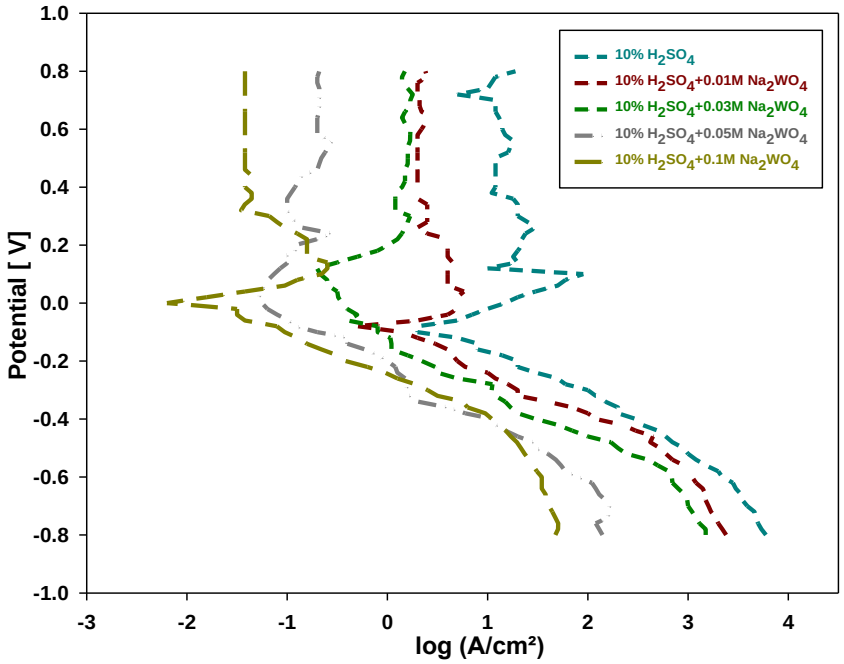

Figure 4. Potentiodynamic polarization curves for Fe-base alloy in 10 % H_2SO_4 solutions in the presence and absence of different concentrations of $Na_2WO_4 \cdot 2H_2O$

Table 5. Corrosion parameters for Fe-base alloy in 10 % H_2SO_4 solutions in the presence and absence of various concentrations of $Na_2WO_4 \cdot 2H_2O$.

Inhibitor Conc. M	E_{corr} V	I_{corr} µA/cm^2	β_a V/dec	β_c V/dec	R_p Ωcm^{-2}	CR,µm/y	θ	IE %
10 % H_2SO_4	-0.087	11.220	0.150	0.160	2.99	87.58	--	--
10 % H_2SO_4+0.01M Na_2WO_4	-0.092	2.512	0.120	0.320	150.8	19.61	0.776	77
10 % H_2SO_4+0.03M Na_2WO_4	0.119	0.251	0.400	0.222	2469.7	1.95	0.977	97
10 % H_2SO_4+0.05M Na_2WO_4	0.078	0.126	0.480	0.286	6176.1	0.98	0.988	98
10 % H_2SO_4+0. 1M Na_2WO_4	0.001	0.039	0.250	0.160	10862.2	0.31	0.996	99

When the concentration of this inhibitor was increased, the inhibition protection increased while the corrosion current densities and corrosion rate decreased. Generally, corrosion current density I_{corr} could reflect the reaction rate. The smaller the I_{corr}, the slower the corrosion rate [13]. This inhibitor cause change in the anodic and cathodic Tafel slopes and no definite trend was noted in the shift of E_{corr} values in the different concentrations of this inhibitor, suggesting that this compound behaves as mixed-

type inhibitors. The values of the Tafel slope ($ß_c$ and $ß_a$) for the inhibitor were shifted slightly which suggested that the investigated inhibitor is blocking the cathodic and anodic sites without changing the corrosion mechanism [19, 20]. The result revealed that Na_2WO_4 is an efficient corrosion inhibitor in 10 % H_2SO_4 solutions to increase the corrosion resistance properties of the Fe-base alloy.

3.3 Surface Morphologies

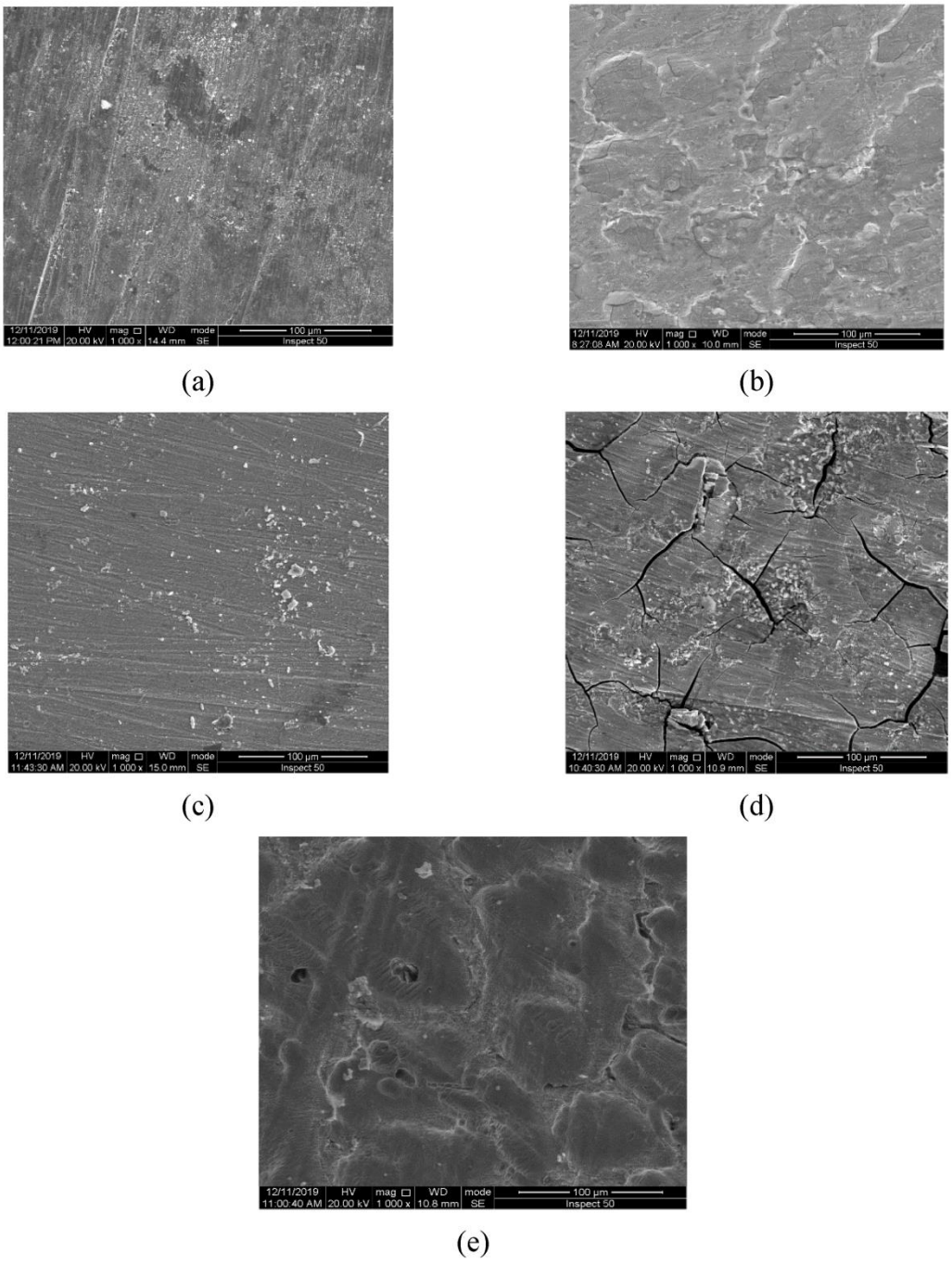

Figure 5. The SEM morphologies of the Fe-base alloy in (a) 5% H_2SO_4 solution, (b) 10%H_2SO_4 solution, (c) 10%H_2SO_4 solution with 0.01 M Na_2WO_4, (d) 10%H_2SO_4 solution with 0.05 M Na_2WO_4 and (e) 10%H_2SO_4 with 0.1 M Na_2WO_4

The SEM morphologies of the Fe-base alloy in concentrations (5%-10%) of H_2SO_4 and different addition of Na_2WO_4 are presented in Fig. 5. Fig. 6 illustrates the EDAX analyses of the Fe-base alloy in 5% H_2SO_4 solution as 23.42%O, 1.12%S, 8.68%Cr, 0.42%Mn, 27.52%Fe, 4.34%Ni and 34.50% W where the EDAX analysis of the alloy in 10% H_2SO_4 solution was 27.45%O, 1.77%S, 3.2% Si, 12.49% Cr, 20.01% Fe, 4.75% Ni, 4.21% Cu and 26.12% W.

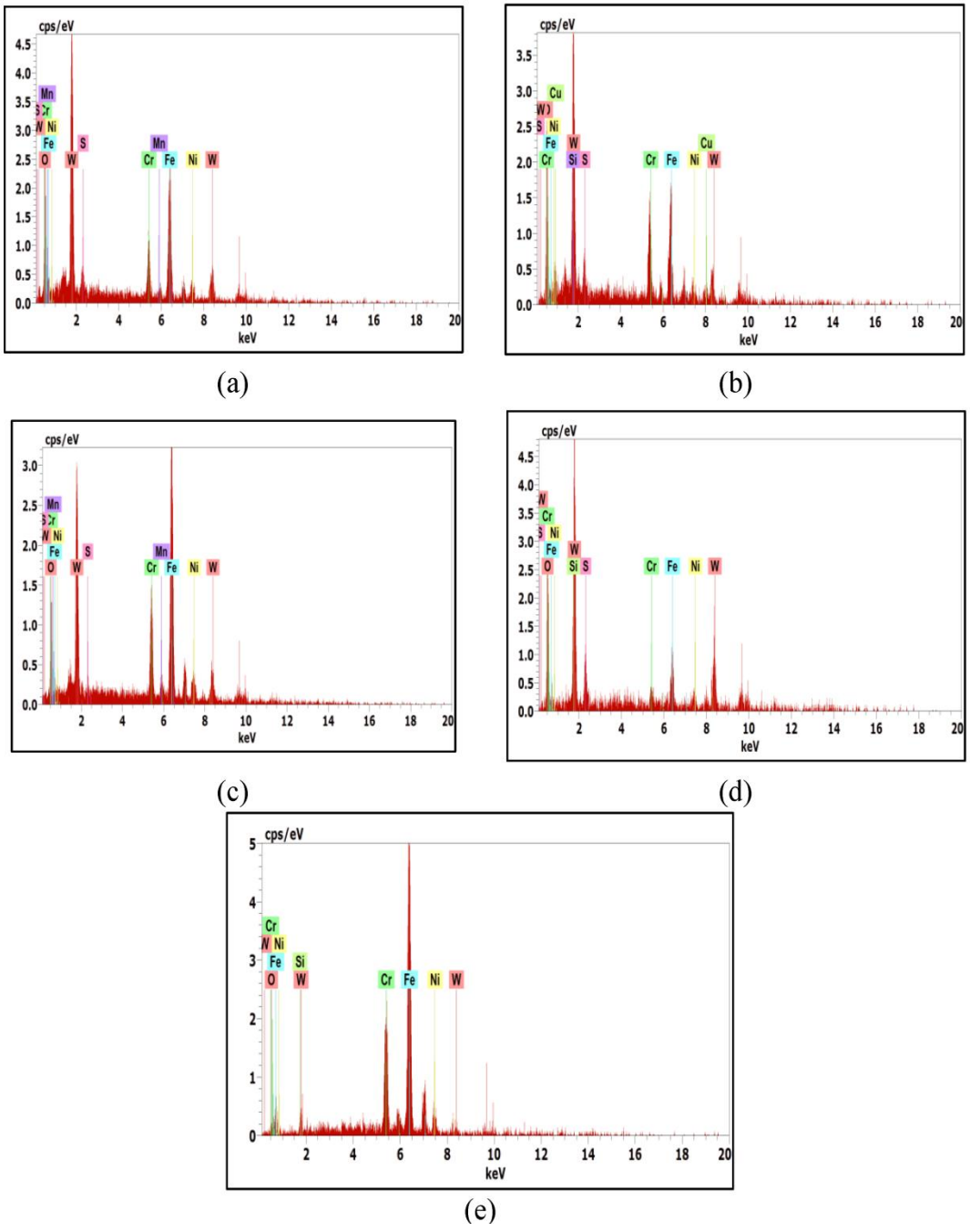

Figure 6. The EDAX analyses of the Fe-base alloy in (a) 5% H_2SO_4 solution, (b) 10% H_2SO_4 solution, (c) 10% H_2SO_4 solution with 0.01 M Na_2WO_4, (d) 10% H_2SO_4 solution with 0.05 M Na_2WO_4 and (e) 10% H_2SO_4 with 0. 1 M Na_2WO_4

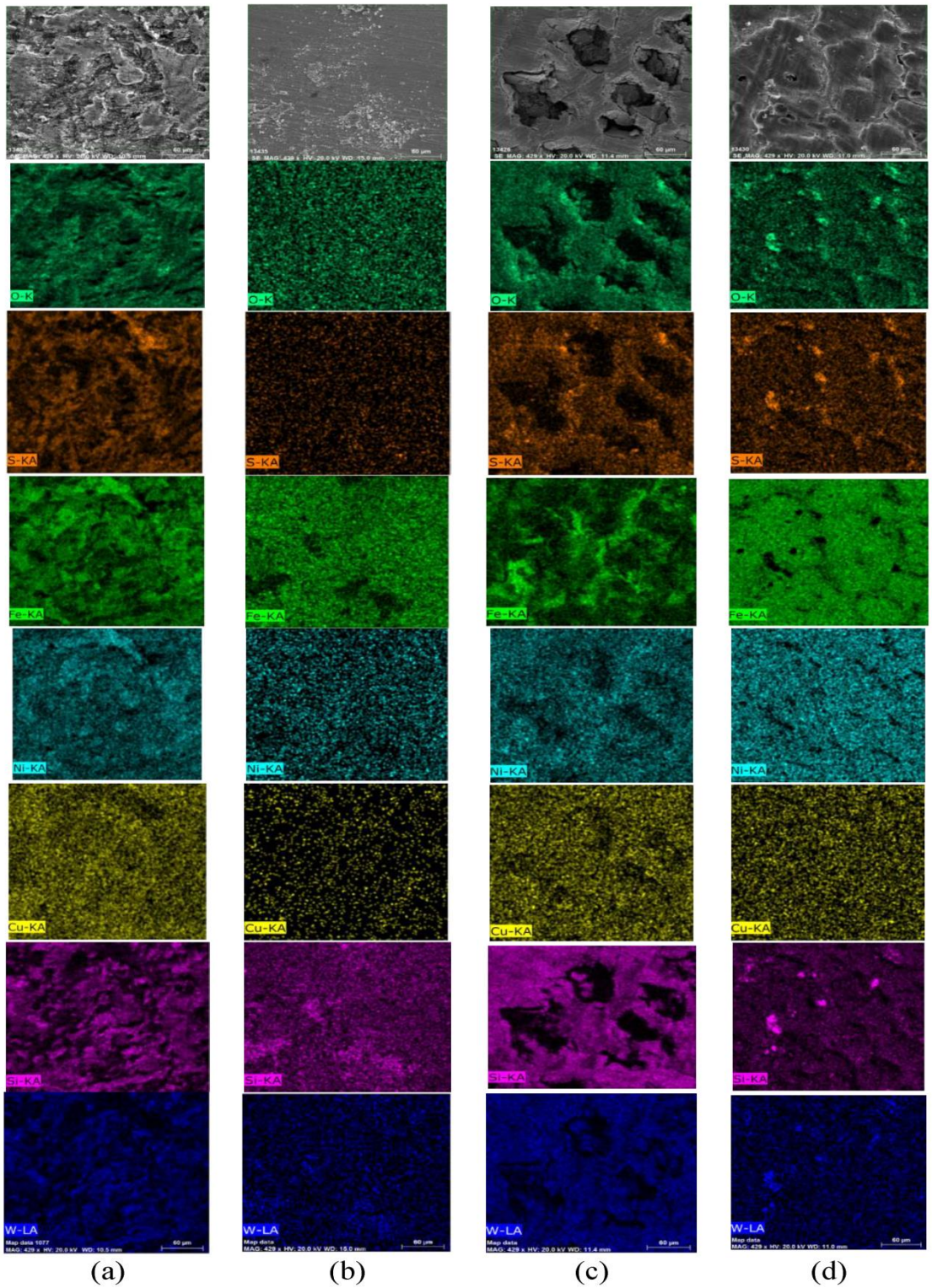

Figure 7. The mapping of the Fe-base alloy in (a) 10% H_2SO_4 solution, (b) 10% H_2SO_4 solution with 0.01 M Na_2WO_4, (c) 10% H_2SO_4 solution with 0.05 M Na_2WO_4 and (d) 10% H_2SO_4 with 0. 1 M Na_2WO_4

The EDAX results of the alloy in 10% H_2SO_4 solution with 0.01 M Na_2WO_4 was10.34% O, 0.3% S, 12.56% Cr, 0.15% Mn, 45.38% Fe, 5.29% Ni and 25.98% W where the EDAX showed the alloy composition in 10% H_2SO_4 solution with 0.05 M Na_2WO_4 to have 27.75% O, 5.25% S, 0.07% Si, 2.19% Cr, 10.48% Fe, 2.08% Ni and 52.18% W. Similarly, the EDAX analysis of the alloy in 10% H_2SO_4 solution with 0.1 M Na_2WO_4 was 0.63% O, 0.33%Si, 18.88%Cr, 70.05%Fe, 6.0%Ni and 4.11%W. The mapping of the Fe-base alloys in concentrations of H_2SO_4 (5%-10%) and different addition of Na_2WO_4 was given in Fig. 7. The presented EDAX analysis results show that when the Fe-base alloy corroded, a concentration of the tungstate occurs at the surface without the addition of the Na_2WO_4 in the H_2SO_4 solution. After the addition of the Na_2WO_4 in the H_2SO_4 solution, the formation of a protective layer on the surface decreased the corrosion rate as illustrated in Fig. 5 and Fig. 7. For 0.05 M Na_2WO_4 in H_2SO_4 acid solution, it is clear from the mapping that the surface corroded through the uncovered areas of the inhibitions, Fig. 7c. Increasing the inhibitor concentration to 0.1 M of Na_2WO_4 in H_2SO_4 acid solution decreased the pits and increases the surface protection as provided in Fig. 7d. The formation of the complex iron – tungstate on the surface is primarily responsible for the inhibition effect that emerged after 1200 ppm [12] concentration. Several particles appeared as a smaller flaky layer, and the tiny cracks vanished, though the surface still contained few pits. In summary, the addition of a higher concentration of Na_2WO_4 effectively prevents the corrosion of Fe-Base alloy in 10% H_2SO_4 solution compared to lower concentration.

4. CONCLUSIONS

The corrosion of Fe-base alloy was evaluated at varying concentrations (1%-10%) of H_2SO_4 solution. The effect of sodium tungstate in 10% H_2SO_4 solution on the corrosion features of Fe-Base alloy was investigated as well. The sodium tungstate acted as good corrosion inhibitors to increase the corrosion protection for Fe-base alloy in the 10 % H_2SO_4 solution. The inhibition efficiency, as concluded from the weight loss tests was 97%, which is in good agreement with that achieved from the tests of potentiodynamic polarization (99%). An inhibitor concentration of 0.1 M Na_2WO_4 was found to be ideal and most efficient. The lowest corrosion density was found at a concentration of 0.1 M of Na_2WO_4, being 0.039 $\mu A/cm^2$, which is significantly lower than that of the blank 10 % H_2SO_4 (11.220 $\mu A/cm^2$). The results obtained from the weight loss tests were in agreement with these obtained from the potentiodynamic polarization results. After the addition of the Na_2WO_4 to the H_2SO_4 solution, the formation of a protective layer on the Fe-Base alloy surface decreased the corrosion rate as concluded from the surface analyses performed by SEM, EDAX, and mapping.

ACKNOWLEDGMENT
The authors gratefully acknowledged the support from the Department of Chemistry, Faculty of Science (Girls), Al-Azhar University, the Department of Mining, Petroleum, and Metallurgical Engineering and Faculty of Engineering, Cairo University.

References

1. S. H. Zaferani, M. Sharifi, D. Zaarei, and M. R. Shishesaz, *J. Environ. Chem. Eng*., 1(4) (2013) 652-657.
2. A. Noh and H. Park, *IFAC-papers online*, 48(17) (2015) 39-41.
3. J. Hu, T. Wang, Z. Wang, L. Wei, J. Zhu, M.Zheng, and Z. Chen, *Coatings*, 8(2018) 315
4. A.K. Satpati and P.V. Ravindran, *Mater. Chem. Phys*., 109(2) (2008) 352-359
5. S. T. Selvi, V. Raman, and N.Rajendran, *J. Appl. Electrochem*., 33 (2003) 1175–1182
6. I. Fouda and A. Ellithy, *Corros. Sci*., 51 (2009) 868–875.
7. N. Obi-Egbedi, I. Obot, and M. I. El-Khaiary, *J. Mol. Struct*.,1002 (2011) 86–96.
8. M. Finšgar and J. Jackson, *Corros. Sci*., 86 (2014) 17–41.
9. I. Berisha, F.Podvorica, V. Mehmeti, F. Syla, and D. Vataj, *Maced. J. Chem. Chem. Eng*., 34(2015) 287–294.
10. F. Mohsenifar, H. Jafari, and K. Sayin, *J. Bio.Tribo.Corros*., 2(1) (2016) 1–13.
11. S. E. Sanni, A. P. Ewetade, M. E. Emetere, O. Agboola, E. Okoro, S. J. Olorunshola, T. S. Olugbenga, *Mater. Today Commun*., 19 (2019) 238–251.
12. M. Javidi, R. Omidvar, *J. Mol. Liq*., 291 (2019) 111330
13. J. Zhang, L. Zhang, G. Tao, and F. Cui, *Int. J. Electrochem. Sci*., 13 (2018) 6522 – 6536.
14. R. Khandelwal, S.K. Arora, S.P. Mathur, *Egypt. J. Chem*., 2011, 3, 1200-1205.
15. H.B. Lokesh, S.P. Fakrudeen and V.B. Raju, *IOSR-JHSS*., 19(6) (2014) 9–20.
16. H. Tang, T. Wu, F. Xu, W. Tao, and X. Jian, *Int. J. Electrochem. Sci*., 12 (2017) 1377-1388.
17. W. Tu, Y. Cheng, T. Zhan, J. Han, and Y. Cheng, *Int. J. Electrochem. Sci*., 12 (2017) 10863 – 10881
18. E. Geler andD.S. Azambuja, *Corros. Sci.* 42(4) (2000) 631–643.
19. A.I. Ali, N. Mohamed, and E.M. Mabrouk, *J. Basic Environ. Sci*., 5 (2018) 306-309
20. Y.Gao, J. Hu, J.Zuo, Q. Liu, H. Zhang, S. Dong, R. Du, and C. Lin, *J. Electrochem. Soc.,* 162 (10) (2015) C555-C562.